Low Temperature Plasma for Astrochemistry: Toward a Further Understanding with Continuous and Precise Temperature Control[*)]

Yu Yu PHUA, Noritaka SAKAKIBARA, Tsuyohito ITO and Kazuo TERASHIMA

The University of Tokyo, 5-1-5 Kashiwanoha, Kashiwa, Chiba 277-8561, Japan

(Received 14 April 2020 / Accepted 13 May 2020)

Astrochemistry is concerned with understanding the chemical evolution in the universe. Despite the harsh and unfavorable conditions, active organic syntheses occur throughout the universe. Laboratory experiments that simulate the conditions of the target astrophysical environment have been used to study the nature and abundances of molecules. In such laboratory simulations, discharge plasma can be used to simulate the energetic processes that occur in the universe. We review the use of discharge plasma in the domain of astrochemistry by considering Titan as an example. Additionally, we discuss the necessity for a plasma source whose temperature can be well controlled at ranges below room temperature (300 K) to simulate the low temperatures that are representative of astrophysical environments. Finally, we present a recent advancement achieved by our group in using cryoplasma, whose temperature can be controlled in a continuous and precise manner below room temperature, to simulate the chemical processes that occur on the surfaces of icy bodies in the outer solar system.

Keywords: cryoplasma, astrochemistry, low-temperature, plasma-ice interface, outer solar system

DOI: 10.1585/pfr.15.1506041

1. Introduction

Life on Earth is based on the chemistry of carbon, which may have been directly inherited from the stars. Elements are created in the heart of stars via nucleosynthesis, and such elements are ejected into the universe when stars explode. These elements undergo further reactions to form complex organic molecules (organic molecules with six or more atoms are termed complex organic molecules in the domain of astrochemistry [1]), which become the source materials from which planets are formed. Therefore, the formation and destruction of molecules in the universe are interesting, as both these phenomena are related to the evolution of stellar and planetary systems and, hence, to the origin of life on Earth as well. Notably, these resulting organic molecules may also initiate life elsewhere in the universe [2–4].

The domain of astrochemistry is concerned with understanding the chemical evolution in the universe. Despite the low-temperature and low-pressure conditions, active organic syntheses are thought to occur in various astrophysical environments such as the follows: (1) the interstellar medium, where stars form [5–7], (2) in planetary atmospheres and surfaces [8, 9], and (3) in comets, and icy bodies in the outer regions of the solar system [10, 11]. The energy deposition from radiation sources such as ultraviolet (UV) radiation is considered to be a dominant mechanism for the formation of complex organic molecules in the universe (see Fig. 1), where conditions that are not favorable to chemistry dominate [4].

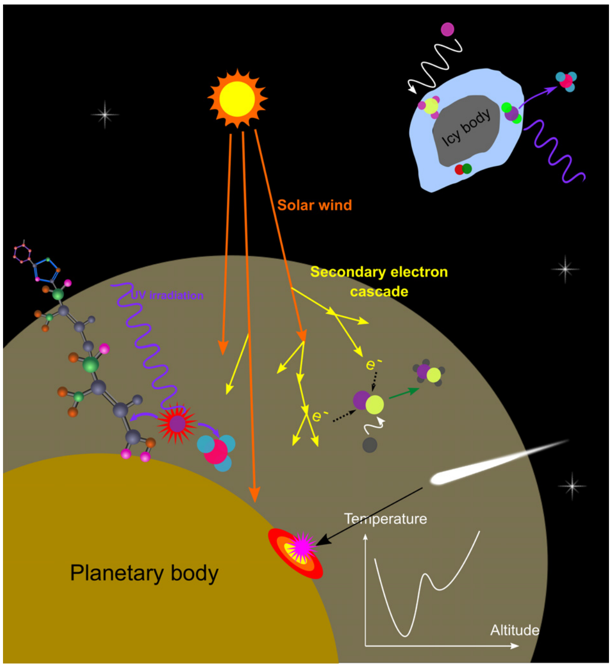

Fig. 1 Image diagram of astrochemistry in various arbitrary astrophysical environments, such as in the atmosphere of a planetary body and on the surface of an icy body.

Currently, the following three major methods are used to study the nature and abundances of molecules in astrochemistry [9, 12, 13]: (1) remote observation or in situ sampling of atmospheric and surface materials, (2) theo-

---

author's e-mail: yuyu@plasma.k.u-tokyo.ac.jp

[*)] This article is based on the invited talk at the 36th JSPF Annual Meeting (2019, Kasugai) retical modeling of the kinetics and dynamics of chemical reactions, and (3) laboratory experiments that simulate the conditions of the target astrophysical environment. Extensive laboratory experiments have been performed to investigate the chemical modifications induced by radiation and to study the nature and abundances of molecules in the universe. In such experiments, conditions such as energy sources, physical parameters including temperature and pressure, as well as the use of reactants that are analogous to the target astrophysical matter, are simulated.

A close simulation of the astrophysical environment is, however, difficult to implement because of complexities of the environment such as exposure to multiple radiation fields including high-energy protons, UV photons, and X-rays, as well as complex surface or atmospheric composition [14, 15]. In addition, the physical parameters, such as temperature, pressure and particle density, which influence collisional processes, vary widely across different astrophysical environments. For example, the interstellar medium span a wide range of densities (10^2 - 10^8 H (hydrogen) atoms cm^{-3}) and temperature (10 - 10^4 K) [6]. The mean free path of molecules in interstellar clouds with density of 10^6 H atoms cm^{-3} and temperature of 10 - 100 K is approximately 10^9 - 10^{15} cm, giving the time between collisions of about 10^4 - 10^{10} s [16]. Among the planets of the solar system, the temperature of the atmosphere can range from 100 K to 1000 K, and the pressure from 10^{-7} to 10^7 Pa [17]. The mean free path of molecules at an altitude of 50 km in Earth's atmosphere, where the number density is 2×10^{16} molecules cm^{-3} and temperature 270 K [18] is $\sim 10^{-5}$ m, giving the time between collisions of about $\sim 10^{-7}$ s [18]. As the degree of molecular interactions is influenced by the simulation of physical parameters which vary over large orders of magnitudes, the applicability of laboratory simulations to astrophysical environments is difficult to achieve. Nevertheless, laboratory simulations are useful to improve our knowledge regarding the chemical evolutions in the universe, especially when observational approaches suffer from technical detection limitations. In addition, laboratory simulations have demonstrated the formation of various complex organic molecules that have been observed in the cosmos, as well as potential species that have yet to be detected [19–21]. These insights are useful to provide realistic constraints for both observational instruments and theoretical models.

In laboratory simulations, various energy sources can be used to drive chemical reactions, depending on the phenomena or environment to be studied. Interstellar ices, planetary bodies, and outer solar system icy bodies are exposed to energetic photons, electrons, and ions that originate from various radiation sources such as cosmic rays, solar wind, magnetospheric particles, and UV radiation. These primary radiation sources often contain highly energetic charged particles. For example, cosmic rays mainly comprise protons that have kinetic energies in the MeV range [22], while solar wind mainly comprises protons that typically have energies in the keV range [23]. To simulate such high-energy radiations, studies have employed gamma radiation [9, 24] as well as various high-energy charged particle beams [25] such as keV~MeV proton beam [19, 26], ~keV He^+ ions [27], and high-energy electron beams [23]. Other than primary radiation sources, low-energy secondary electrons (< 15 eV [4, 9, 28]) that are produced from the interaction of high-energy radiation with matter such as gaseous molecules and cosmic ices, can also induce chemical processes in the universe. The effects of low-energy secondary electrons can be simulated using low-energy electron beams [28, 29], as well as non-equilibrium low-temperature discharge plasma [9], in which the mean electron temperature is often <10 eV. While the effects of UV radiation can be simulated with UV lamps [25], non-equilibrium low-temperature discharge plasma can also be used to simulate UV irradiation [9].

In this review, we focus on the use of discharge plasma for simulating chemical processes that specifically occur on the surfaces or atmospheres of solar system bodies. In the next section, the use of discharge plasma in astrochemistry is described using Titan, which is an icy body whose chemistry has been extensively studied, as an example. Notably, Titan possesses a nitrogen-dominated atmosphere and, hence, presents an active chemistry. However, a shortcoming of using discharge plasma is the difficulty in simulating the cryogenic-temperature conditions that are found in numerous environments in the universe. This difficulty is posed because the gas temperature of low-temperature plasma is barely below room temperature. The necessity for a plasma source whose temperature can be well controlled at ranges below room temperature, as well as several attempts made to simulate the low-temperature condition found in astrophysical environments, are discussed in Sec. 3. Subsequently, we describe a recent approach devised by our group of using cryoplasma to simulate the chemical processes that occur on icy bodies in the outer solar system.

2. Laboratory Simulations of Chemistry by Using Discharge Plasma, with Titan as an Example

Titan is the largest moon of Saturn. Some physical and orbital parameters of Titan are shown in Table 1. The temperature and pressure profile of Titan are shown in Fig. 2. The surface temperature of Titan is approximately 94 K [30], which is much colder than Earth. The temperature decreases with altitude to approximately 70 K at the minimum, and then increases to approximately 180 K at the altitude of 250 km up the atmosphere. On the other hand, Titan's surface pressure is approximately 1.5 times that of Earth, at 1.467×10^5 Pa.

Table 1 Physical and orbital parameters of Titan. All values are taken from [31] unless otherwise stated in the table.

Property	Value
Mass	1.35×10^{23} kg (= 0.022× Earth)
Distance from Saturn	1.23×10^{9} m
Distance from Sun	9.546 AU
Rotation period	15.95 days [30]
Orbital period around Saturn	15.95 days
Orbital period around Sun	29.5 years
Surface temperature	93.65 K
Surface pressure	1.467×10^{5} Pa
Surface gravity	1.354 m s^{-2}
Solar flux at top of atmosphere	3.7 W m^{-2} [32]
Internal magnetic field	none detected [33]

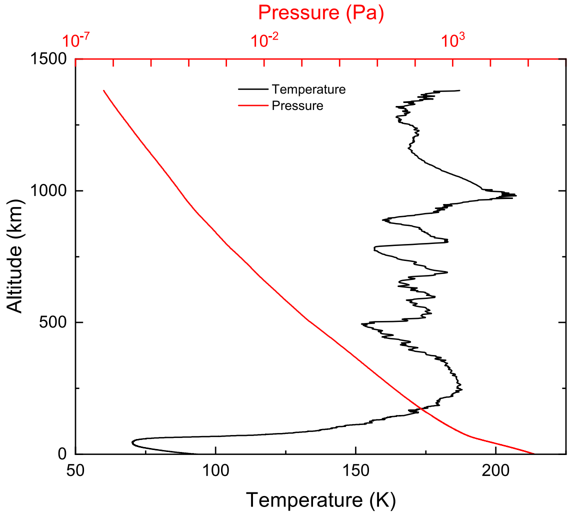

Fig. 2 The pressure and temperature with altitude of the atmosphere of Titan as determined by Huygens Atmospheric Structure Instrument on board the spacecraft Huygens in the Cassini-Huygens mission [69].

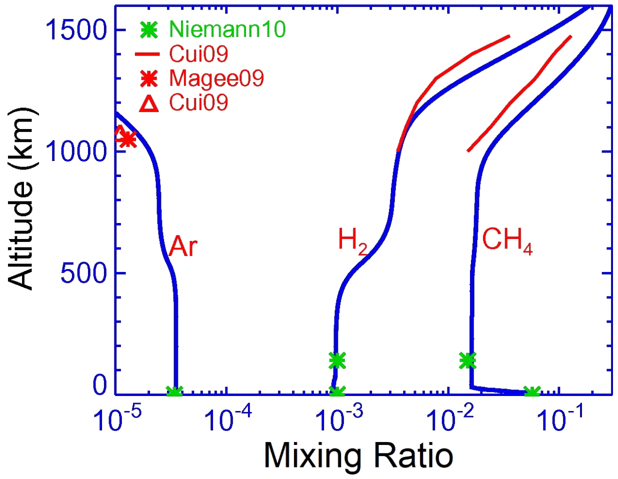

Fig. 3 Vertical distribution of the mixing ratios of Ar, H_2 and CH_4 based on calculated models (solid blue line) and observational data (from [39–41]). Reproduced with permission from [42], copyright 2014 Elsevier.

Titan has a dense atmosphere that mainly comprises nitrogen (95% - 98%), a low percentage of methane, hydrogen, and argon, with trace amounts of hydrocarbons and nitriles including C_6H_6 and HCN (see Fig. 3, Fig. 4, and Table 2). The nitrogen-dominated atmosphere of Titan makes it a unique planetary body in the solar system. The ongoing chemical processes in the atmosphere due to solar UV and Saturn's magnetospheric electrons drive the formation of various complex organic molecules, such as hydrocarbons and nitriles [34]. Some of these organic molecules could lead to the formation of molecules of prebiotic interests [30].

The mole fractions of minor species are seen to increase with altitude (see Fig. 4), indicating that such minor species are produced by photochemistry at high altitudes, and subsequently condense at the lower atmosphere [30]. Through further chemical processes, these hydrocarbons and nitriles form solid organic aerosols that are reddish-brown. The reddish-brown solid organic aerosols are thought to give rise to the reddish color of Titan [35]. The processes that result in the formation of aerosols in the atmosphere of Titan are depicted in Fig. 5. To investigate the mechanisms and dynamics of the chemistry occurring in the atmosphere of Titan, many studies have simulated the physical and chemical conditions of the atmosphere of Titan in the laboratory [36–38]. In such studies, the analogs of Titan's organic aerosols, which contain various hydrocarbons and nitrogen-containing compounds, were synthesized, in solid forms, as well as deposited as films (see Fig. 6).

Energetic sources into Titan's atmosphere include solar photons, electrons and protons from the sun and the magnetosphere of Saturn, and galactic cosmic rays. The fluxes and energy of these sources are shown in Fig. 7 (a) while the contribution of some of these energetic sources to the production of ions as a function of altitude are shown in Fig. 7 (b). Most high energy electrons, protons and photons are attenuated by the molecules in the atmosphere below 600 km, while ~99% of solar photons of longer wavelengths (> 220 nm) can penetrate to lower altitudes of about 100 km above the surface. For example, at an altitude of 200 km, the solar flux at 220 nm is $\sim 1 \times 10^{10}$ photons cm^{-2} nm^{-1} s^{-1} while that of 350 nm is one order of magnitude larger at $\sim 3 \times 10^{11}$ photons cm^{-2} nm^{-1} s^{-1} [43].

From Fig. 7 (b), we see that solar UV photons are a major primary ionization source in Titan's atmosphere. Not only solar UV photons but also other primary ionization sources such as magnetospheric electrons interact with gaseous molecules in the atmosphere and produce low-

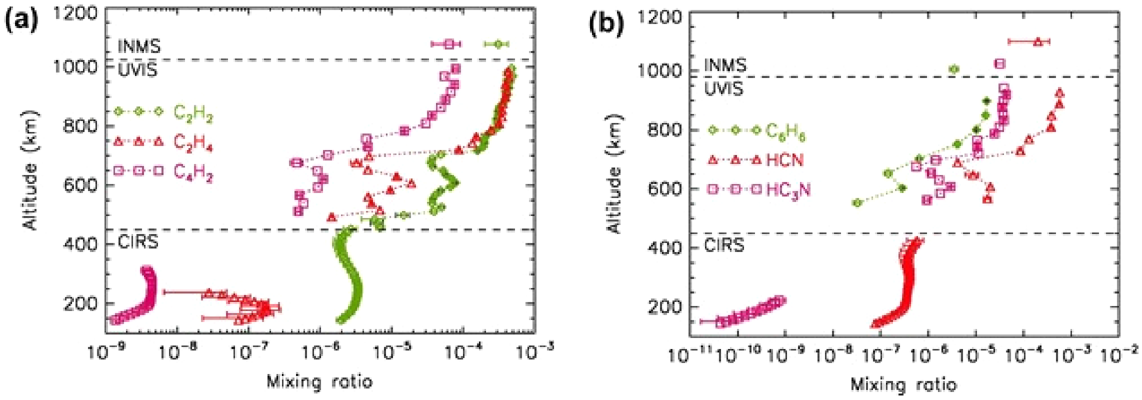

Fig. 4 Vertical distribution of the mixing ratios for various minor species based on data obtained by instruments on board the spacecraft Cassini in the Cassini-Huygens mission, namely Composite Infrared Spectrometer (CIRS), Ultraviolet Imaging Spectrograph (UVIS), and Ion and Neutral Mass Spectrometer (INMS). Reproduced with permission from [44], copyright 2011 Elsevier.

Table 2 Composition of Titan's atmosphere. All values are taken from [30] unless otherwise stated in the table.

Constituent	*Mixing ratio*		
N_2 [9]	$9.4 - 9.8\times10^{-1}$		
	Stratosphere (~ 200 km)	*Mesosphere* (~ 700 km)	*Thermosphere* (> 700 km)
CH_4 [42]	$1.5 - 5\times10^{-2}$	$\sim 1.5\times10^{-2}$	$1.7\times10^{-2} - 2\times10^{-1}$
H_2	$9.6 \pm 2.4\times10^{-4}$		$3.9 \pm 0.01\times10^{-3}$
C_2H_2	2.97×10^{-6}	$5.9 \pm 0.6\times10^{-5}$	$3.1 \pm 1.1\times10^{-4}$
C_2H_4	1.2×10^{-7}	$1.6 \pm 0.7\times10^{-6}$	$3.1 \pm 1.1\times10^{-4}$
C_6H_6	2.2×10^{-10}	$2.3 \pm 0.3\times10^{-7}$	$8.95 \pm 0.44\times10^{-7}$
HCN	6.7×10^{-8}	$1.6 \pm 0.7\times10^{-5}$	
CH_3CN	$< 1.1\times10^{-7}$		$3.1 \pm 0.7\times10^{-5}$
CO	$4.7 \pm 0.8\times10^{-5}$		
H_2O	$4.5 \pm 1.5\times10^{-10}$		$< 3.42\times10^{-6}$
CO_2	1.1×10^{-8}		$< 8.49\times10^{-7}$

energy secondary electrons (< 15 eV) (see Fig. 1), whose effects can be simulated by using discharge plasma. In the rest of this section, we briefly overview the manner in which discharge plasma has been used for more than 30 years to simulate the chemistry in the atmosphere of Titan that is induced by UV photons and low-energy secondary electrons (for a comprehensive review of all the relevant research on the laboratory simulations of Titan's atmospheric chemistry, readers are referred to a recent review article by Cable *et al.* (2012) [9]).

While chemistry induced by UV photons from the sun and chemistry induced by electrons may be different, in terms of energy, a Maxwellian electron energy distribution function (EEDF) of 1 - 2 eV is found to have a similar broad spectrum to the solar radiation spectrum, as shown in Fig. 8 (Here, the solar spectrum taken from the top of the Earth's atmosphere at 1 AU is used for comparison with the EEDF. The solar spectrum at the top of Titan's atmosphere is expected to be similar in energy distribution [51].). Although the EEDF of discharge plasma can deviate from a Maxwellian distribution, it is indicated from Fig. 8 that the energy range of electrons in discharge plasma can be crudely approximated to be similar to that of solar photons.

In addition, the electrons in the high-energy tail of the EEDF (> 10 eV) have sufficient energy to dissociate molecular bonds that have high dissociation energies such as N_2 (dissociation energy = 9.76 eV). In contrast, in experiments using UV radiation to simulate the effects of solar UV, molecular nitrogen often cannot be dissociated because UV sources in the far-UV range (i.e., 115 - 200 nm, which corresponds to 6.2 - 10.8 eV) are often used, and the dissociation cross-section of N_2 is low in this wavelength region [52]. Moreover, in experimental setups where silica windows are used, UV radiation above 6.2 eV are blocked out, and, therefore N_2 cannot be dissociated [36]. Accordingly, in such studies, other N-containing reactants, such as HCN, must be used to provide N atoms.

The experimental conditions that were employed in several studies and their respective objectives are summarized in Table 3. It can be seen that the conditions vary widely, and various plasma sources have been used to simulate the irradiation of charged particles and UV radiation: spark discharges [37, 57, 58], dielectric barrier discharges [59], radio-frequency (RF) inductively or capacitively coupled discharge plasma [38, 60–62], and DC discharges [63–65]. The initial gaseous mixture used is most often an N_2-CH_4 mixture with varying CH_4 concentrations, which are frequently in the range of 1% - 10% [36, 65–68].

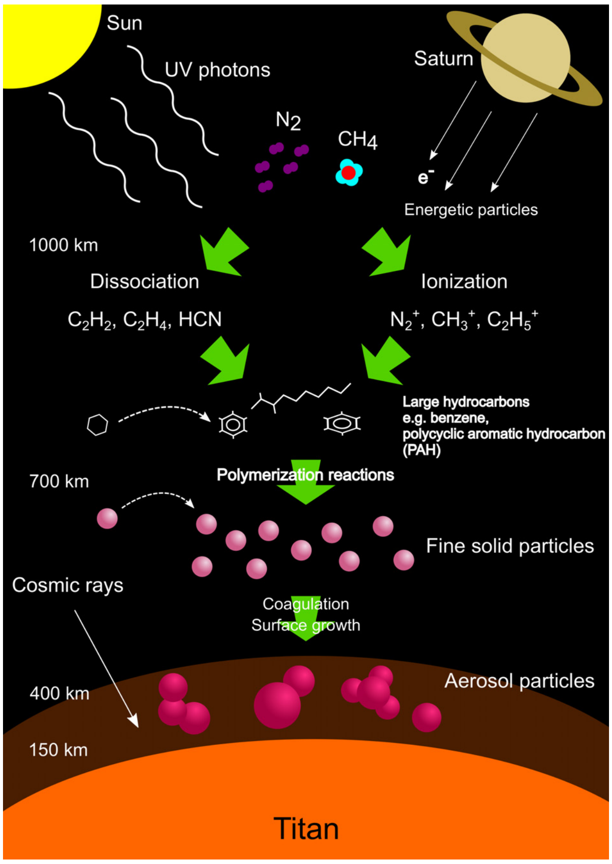

Fig. 5 Aerosol formation process in the atmosphere of Titan. (Modified from [45, 46].)

Other than replicating the sources of energy and gas compositions, it is also important to replicate physical variables such as the temperature, pressure, and wind condition of the environment that are relevant to the formation of the aerosols on Titan. Complex organic chemical reactions that result in the formation of aerosols are expected to initiate at high altitudes near 1000 km [45] (see Fig. 5), where the pressure is approximately 10^{-5} Pa and the temperature lower than 200 K [69]. While the reddish aerosol clouds have been observed to reside primarily at the lower altitudes of 250 km [45, 52], the temperature and pressure at these altitudes remain relatively low at 180 K and 10 Pa, respectively [69]. Such low-pressure condition is not ideal for performing a laboratory experiment, as the frequency of collisions would be considerably small for the reactions to occur and for detectable quantities of prod-

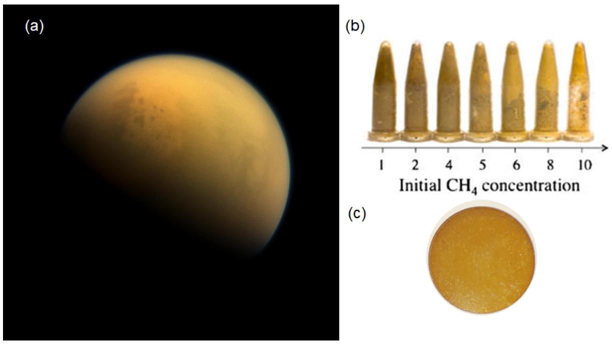

Fig. 6 (a) Photo of Titan (NASA) [47]. (b) Titan aerosol analogs synthesized in the laboratory at various initial methane concentrations [48]. (c) Titan aerosol analog film deposited on quartz disk (diameter: 2.54 cm). Reproduced with permission from [49], copyright 2018 The American Astronomical Society.

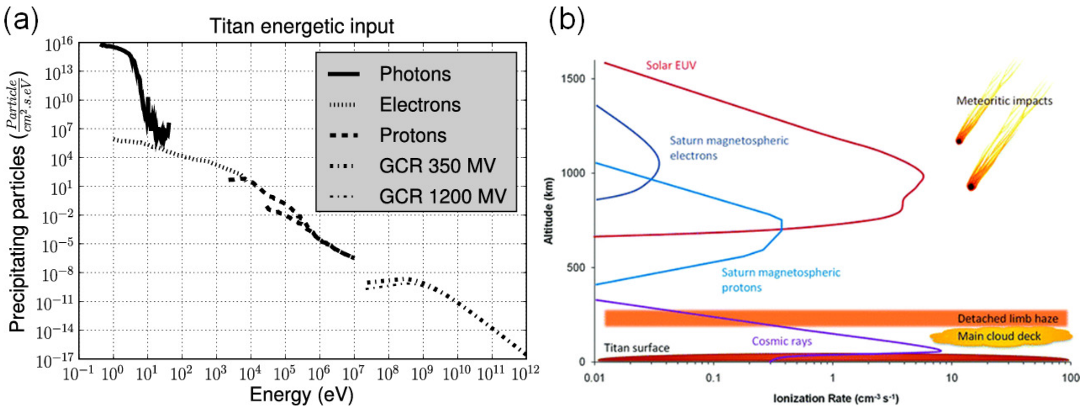

Fig. 7 (a) Fluxes of energetic sources into Titan's atmosphere including solar photons, electrons and protons from the sun and the magnetosphere of Saturn, and galactic cosmic rays (GCR). Reproduced with permission from [50], copyright 2009 European Southern Observatory. (b) Ionization rates of various energetic sources in Titan's atmosphere as a function of altitude. Reproduced with permission from [9], copyright 2011 American Chemical Society.

Table 3 Experimental conditions employed in several studies that were based on the synthesis of Titan's organic aerosols by using discharge plasma.

Reference	Plasma source	Initial gas mixture	Temperature	Pressure	Irradiation time	Yield of aerosol analogs	Purpose
Coll *et al.* (1999) [96]	DC discharge	98:2 N_2:CH_4	100 - 150 K	200 Pa	8 h		Detection of C_4N_2 in simulation of Titan's atmospheric chemistry
Thompson *et al.* (1991) [60]	RF discharge	90:10 N_2:CH_4	295 K	1.7×10^3 Pa	49 h 34 m		Effect of pressure on Titan chemistry
	RF discharge	90:10 N_2:CH_4	295 K	24 Pa	49 h 17 m		
McKay (1996) [57]	Spark discharge	90:10 N_2:CH_4	300 K	1.15×10^5 Pa	21 days	Solid of several hundred mg	Determination of physical, optical and chemical properties of aerosol analogs
Bernard *et al.* (2003) [64]	DC discharge	98:1.99:0.01 N_2:CH_4:CO	350 - 450 K	10^2 Pa	50 h		Effect of CO on Titan chemistry
Sciamma-O'Brien *et al.* (2012) [61]	RF discharge	95:5 N_2:CH_4	300 K	90 Pa	2 h	Film thickness 0.42 µm	Characterization of optical constants of aerosol analogs
Poch *et al.* (2012) [65]	DC discharge	98:2 N_2:CH_4	170 K	10^2 Pa	11 - 16 h	Solid of ~10 mg	Production of astrobiologically interesting molecules from aerosol analogs
Mahjoub *et al.* (2014) [62]	RF discharge	N_2 + 1~5% CH_4	105 K	90 Pa	2 h	Film thickness 0.53 - 0.75 µm	Effects of temperature on optical and chemical properties of aerosol analogs

ucts to be formed in a realistic time frame. Therefore, higher pressure that is frequently of approximately 10^2 Pa is used [62, 65, 68, 70]. On the other hand, with regards to temperature, because of the difficulties of maintaining cryogenic temperatures, most experiments have been conducted at room temperature, which is significantly higher than that of the atmosphere of Titan [36, 66, 71].

As for the wind conditions, according to Fig. 9 (a), in the troposphere (~40 km), eastward zonal winds of 0.5 to 10 m s^{-1} have been observed. In the stratosphere, super-rotating winds with speeds of up to 200 m s^{-1} have been detected. The zonal wind speed subsequently decreases to about 60 m s^{-1} near altitude of 450 km. On the other hand, in the lower troposphere, there is a southerly wind peaking at 0.9 m s^{-1} below altitude of 1 km, and a northerly wind peaking at 0.4 m s^{-1} above 1 km (see Fig. 9 (b)). Such atmospheric dynamics have a feedback on the chemistry, aerosol growth and distribution, and composition of the atmosphere as particles are transported vertically and horizontally across the atmosphere by atmospheric dynamics. However, while climate models that couple atmospheric dynamics, atmospheric compositions, and chemistry have been developed [72–74], atmospheric dynamics are not often considered in laboratory simulations of the chemical processes occurring in the atmosphere of Titan.

Although the current laboratory simulations have not been able to perfectly replicate the environment, as well as all the phenomena observed in the atmosphere of Titan, many compounds that have been observed in the atmosphere of Titan have been reproduced in the laboratory [12, 89]. Therefore, it can be said that to some extent, the chemical pathways that result in the formation of aerosols in Titan can be reproduced using laboratory simulations.

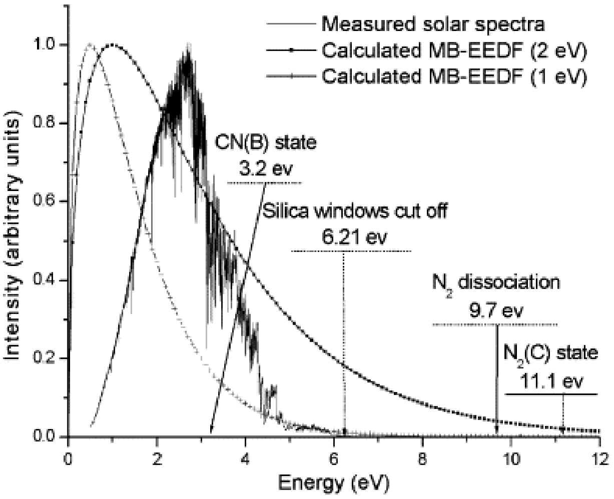

Fig. 8 Maxwell Boltzmann EEDF with electron temperature of 1 and 2 eV, compared with the measured solar spectrum in terms of photon energy. Reproduced with permission from [36], copyright 2006 Elsevier. The measured solar spectrum was built from data from the first Atmospheric Laboratory for Application and Science mission (ATLAS 1) (for UV and visible range) and European Retrievable Carrier mission (EURECA) (for infrared range) [53]. The data from ATLAS 1 were obtained when the space shuttle was oriented toward the sun [54] during the ten-day mission between 24 March, 1992 and 2 April, 1992, a period of moderately high solar activity (solar radio flux *F*10.7 monthly mean of 171 units). During this mission, the space shuttle was in an orbit of approximately 296 km altitude on average [55]. The data from EURECA were obtained in September - October 1992, a period of lower solar activity (*F*10.7 of 132 units) than ATLAS 1. The EURECA spacecraft was deployed into the low earth orbit (altitude 508 km) [56].

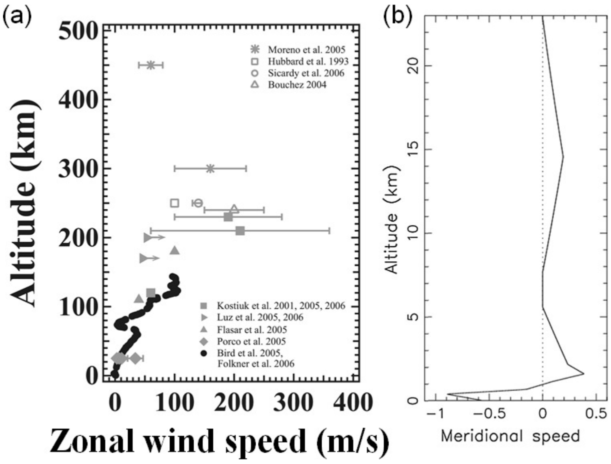

Fig. 9 (a) Vertical profile of zonal wind in the atmosphere of Titan (from [75–87]). Reproduced with permission from [30], copyright 2017 John Wiley & Sons. (b) Meridional wind in the troposphere, with positive values indicating easterly and northerly winds. Reproduced with permission from [88], copyright 2015 Elsevier.

The chemistry in the atmosphere of Titan resulting in the formation of various organic compounds including aerosols, is considered to involve the interactions between hydrocarbons, nitrogen-containing species and possibly also oxygen-containing species [34, 90–92]. However, because of the complexities of the chemical pathways involved, only those initial stages of the chemistry that are considered to result in the formation of aerosols will be examined briefly here. The observational data from the Ion Neutral Mass Spectrometer aboard the Cassini spacecraft suggest that the ion-neutral chemistry in the ionosphere of Titan (~1000 km) is central to forming complex organic compounds that are precursors to the production of aerosols [45] (see Fig. 5). According to the model-based calculations of the ion-neutral chemistry that occurs in the ionosphere of Titan [93], the ionization and dissociation of the neutral constituents, namely, N_2 and CH_4, produce initial ions such as ${N_2}^+$ and ${CH_3}^+$ (reaction 1). These initial ions undergo further ion-neutral reactions that result in the synthesis of light hydrocarbons such as ${C_2H_5}^+$ (reaction 2). Further reactions of these simple cations result in the formation of complex organic molecules and, eventually aerosols.

$$ {N_2}^+ + CH_4 \longrightarrow {CH_3}^+ + H + N_2, \tag{1} $$

$$ {CH_3}^+ + CH_4 \longrightarrow {C_2H_5}^+ + H_2. \tag{2} $$

In some laboratory simulations of the chemical processes occurring in the atmosphere of Titan, the above-mentioned precursor ions, as predicted using calculated models, were detected. Dubois *et al.* (2020) [94] investigated the chemical pathways of cations in a capacitively coupled N_2-CH_4 discharge plasma. In their study, major precursor cations such as ${CH_3}^+$ (m/z 15) and ${C_2H_5}^+$(m/z 29) were detected via mass spectrometry. They suggested that ${CH_3}^+$ was formed in their experiment according to reaction 1. They believed that at relatively higher CH_4 concentrations, ${CH_3}^+$ facilitated the formation of ${C_2H_5}^+$, as shown in reaction 2. These laboratory data are consistent with the above-cited model calculations [93].

The results of Dubois *et al.* (2020) [94] show that discharge plasma can be used in laboratory studies to explore the chemistry of the atmosphere of Titan. Although the recent improvements in photochemical modeling [34, 95] have increased our understanding of the chemical processes that occur in the atmosphere of Titan, we still lack considerable information regarding the specific chemical pathways that result in the production of organic aerosols. Therefore, more research needs to be performed on detecting intermediate ions in laboratory simulations under Titan-like conditions. This will provide important constraints on the potential chemical species that might be involved in the pathways that result in the formation of aerosols. Further experimental improvements, such as a more accurate simulation of the various energy sources deposited in the atmosphere of Titan, simulations at cryogenic temperatures, and detection of intermediate species, are critical to enhancing our understanding of the chemistry of Titan's atmosphere.

3. Necessity for Simulations at Cryogenic Temperatures

As mentioned in the previous section, although discharge plasma can be used in the laboratory to explore the chemistry of the atmosphere of Titan, a shortcoming still remains that most experiments are conducted at room temperature, which is considerably higher not only than that of the atmosphere of Titan but also than that of various other astrophysical environments. This is because currently, the gas temperature of non-equilibrium low-temperature plasma that is used widely in industrial plasma-based processes, as well as in simulating the chemistry that occurs in astrophysical environments [38], remains relatively high at above room temperature. However, it is necessary to perform laboratory simulations at the cryogenic temperatures that are representative of astrophysical environments. This is because temperature is a key factor that affects multiple properties of chemical reactions, such as the thermodynamic stability of products and reactants, and reaction kinetics. For example, dicyanoacetylene (C_4N_2) has been detected in the atmosphere of Titan. This compound is thermally unstable and volatile at room temperature and, hence can only be observed in experiments that are performed at low temperatures [96]. Therefore, performing simulations at representative temperatures enables us to gain a more comprehensive understanding of the chemical processes that occur in various environments in the universe.

One of the simplest methods to generate plasma in cryogenic conditions with gas temperature lower than room temperature in order to simulate cryogenic environments, is to cool the plasma reactor by using a cryogenic fluid such as liquid nitrogen. Several studies have attempted to simulate the cryogenic-temperature conditions of Titan by cooling the plasma reactor using liquid nitrogen [12, 62, 65, 67]. Using this method, Mahjoub *et al.* (2014) [62] synthesized the analogs of Titan's aerosols at the ambient temperature of 105 K, to determine the effects of temperature on the optical constants of the analogs synthesized. On the other hand, Sciamma-O'Brien *et al.* (2014) [97] used a different approach to simulate the low-temperature conditions of Titan to investigate the chemical pathways that result in the production of aerosols in the atmosphere of Titan. In their study, a pulsed supersonic plasma jet expansion was used to cool the gaseous reactants and induce chemistry at an ambient temperature of 150 - 200 K. They confirmed that the gas temperature of N_2 was low in the plasma, with a rovibrational temperature of 210 K.

In addition, temperature can also affect the phases in which the material can exist. Laboratory simulations should be performed in the same phase as that found in the astrophysical environment concerned. Other than gaseous atmospheres such as that of Titan, matters of different phases exist in the universe. In particular, ice is ubiquitous and is a dominant reaction field in the universe [25, 98]. Many planetary bodies, such as Pluto, possess an icy surface, while comets and outer solar system bodies, such as trans-Neptunian objects, are made up of significant amounts of ice [98]. Similar to that in the atmosphere of Titan, radiation-induced chemistry can also occur on such icy objects. For example, it is currently understood that the energetic irradiation of molecules that are adsorbed onto the surface of interstellar ice dust, via sources such as UV radiation and cosmic rays, induce chemistry that results in the formation of complex organic molecules [14]. In experiments that investigate the irradiation of ice samples, it is important that the data is collected at temperatures in which these compounds are present in the solid form, which is the form in which they are present in the universe. A study on the irradiation of icy cometary bodies via discharge plasma was performed by McDonald *et al.* (1996) [99]. In the aforementioned study, an ice sample that contained water, methanol, carbon dioxide, and ethane was irradiated using plasma, with the surroundings cooled to 77 K using liquid nitrogen, to study the chemical compositions of cometary ices.

4. Continuous and Precise Temperature Control at Cryogenic Conditions May Reveal New Phenomena

Although cooling of a reactor by using liquid nitrogen is experimentally simple to implement, it is difficult to control the temperature of the reaction system in a continuous and precise manner. For example, in the study by McDonald *et al.* (1996) [99], the plasma irradiation of the ice sample was conducted at 77 K because of the technicality due to using liquid nitrogen as the coolant. In addition, heating of the plasma can occur because of the discharge current, which subsequently increases the temperature of the reaction system.

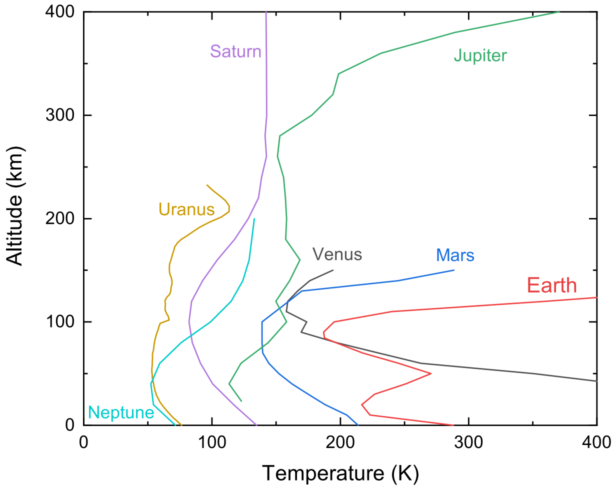

Fig. 10 Temperatures of the atmospheres of various solar system planets as a function of altitude [18, 100–103].

A continuous control of the temperature of the reaction system is needed to simulate the temperature gradient that exists throughout the universe [9]. Temperature gradients are present within individual astrophysical environments such as in the atmospheres of individual planetary bodies, where temperature varies with altitude (see Fig. 10). This temperature variation might cause the reactions rates to change as a function of altitude. As objects move across the universe, the temperature of specific environments, such as the surface temperature of astrophysical objects, can also vary as a function of the heliocentric distance. For example, the calculated surface temperatures of two H_2O-ice bodies that are moving along the orbit of comet Tempel 2 (continuous line) and that of Halley (dashed line) are depicted as a function of the heliocentric distance in Fig. 11. We see that the temperatures of the cometary bodies change in the ranges below room temperature as they orbit around the sun. This temperature change could affect the materials that would remain on the bodies as these icy bodies move across the solar system. Therefore, a low-temperature plasma source that enables the continuous control of the reaction system temperature, at a wide range of temperatures below room temperature, is needed to simulate such temperature gradients. This could provide a more comprehensive understanding of the chemical processes and temperature-dependent chemical evolutions that occur in the universe.

One such plasma source that can be used to simulate the chemistry that occurs in various cryogenic astrophysi-

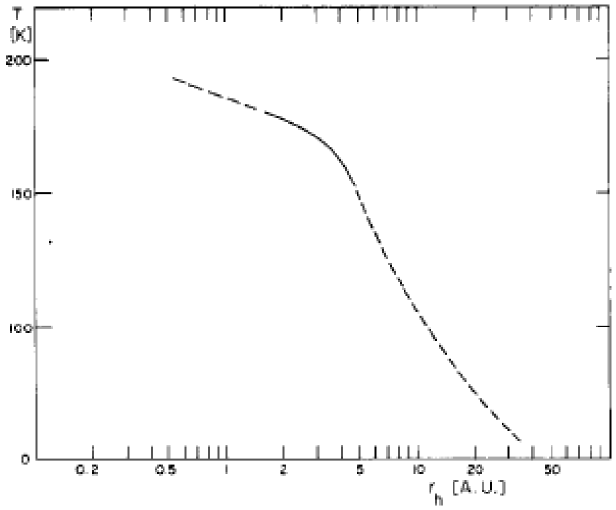

Fig. 11 Calculated surface temperatures, neglecting heat conductions to the interior, of two H_2O-ice bodies that are moving along the orbit of comet Tempel 2 (continuous line) and that of Halley (dashed lines). Reproduced with permission from [104], copyright 1981 Elsevier.

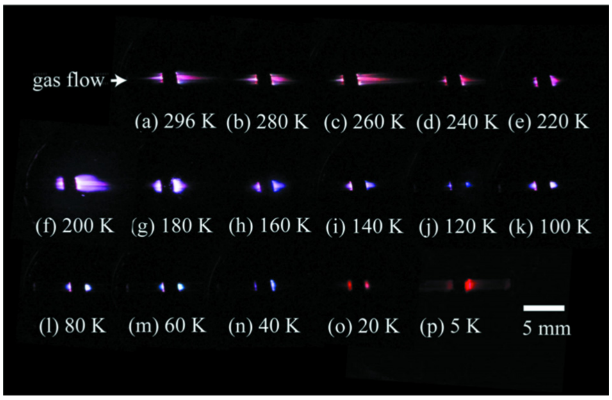

Fig. 12 Helium cryoplasma jet at 296 K to 5 K. Reproduced with permission from [107], copyright 2008 AIP Publishing.

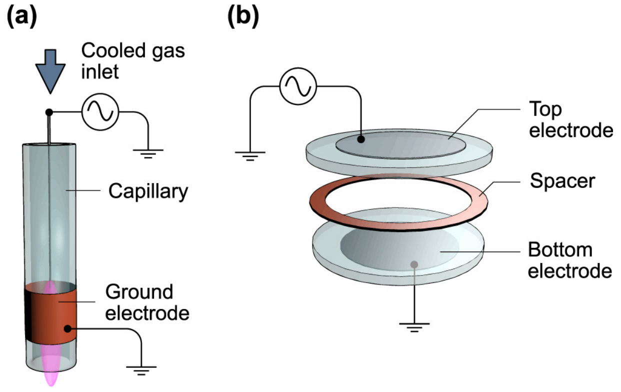

Fig. 13 (a) Schematic illustration of capillary DBD plasma jet. Reproduced with permission from [105], copyright 2018 IOP Publishing. (b) Schematic illustration of coplanar DBD configuration. Reproduced with permission from [105], copyright 2018 IOP Publishing.

cal environments, while achieving continuous and precise temperature control, is cryoplasma, which was developed by our group. Cryoplasma is a non-equilibrium plasma source in which the gas temperature can be controlled continuously below room temperature, demonstrated thus far down to the tens of Kelvin (see Fig. 12). The temperature control can be achieved using a cryostat-equipped temperature control system, by limiting the plasma geometry to less than approximately 1 mm, and limiting the discharge current to minimize the heating of the plasma [105]. A dielectric barrier discharge (DBD), in a plasma jet configuration (see Fig. 13 (a)) and a coplanar configuration (see Fig. 13 (b)), is frequently used to generate a cryoplasma. An example of an atmospheric pressure helium cryoplasma jet generated in open air is depicted in Fig. 14 (a), with the electrode configuration shown in Fig. 14 (b). The plasma gas temperature was estimated using thermocouples, and it was observed to be approximately 230 K. The nitrogen rotational temperature, which was estimated from the optical emission spectra, was approximately 220 K. The air-humidity-induced frost formation around the discharge capillary also substantiates that a cryoplasma with gas temperature considerably lower than room temperature was generated [106]. As the gas temperature decreased from 296 K to 5 K, the color of the cryoplasma jet changed from pink to purple to white to red (see Fig. 12). The change in color reflects how the plasma chemistry changes dynamically with temperature. For example, the emissions of air impurities such as N_2 and O_2 became less prominent as they solidified, while those of He became more dominant [107].

Our group has demonstrated that cryoplasma can coexist with H_2O-ice while achieving good temperature control at 6.5 - 273 K (see Fig. 15) [108]. This is supported by Fig. 16, which indicates that continuous generation of plasma was achieved in the temperature ranges of both liquid and solid H_2O. A change in the discharge mode was observed as H_2O transitioned from the liquid to solid phase, as reflected by the significant decrease in the power consumption near 273 K, which is the melting point of water. The plasma–ice interface created from the coexistence of cryoplasma with H_2O-ice can present a novel interfacial reaction field [108]. The electron flux onto the ice surface was 1.6×10^{15} $\mathrm{cm^{-2}s^{-1}}$, which is of the same order as that of the photon flux of the UV radiation used in the laboratory simulation of UV-irradiated formation of amino acids on interstellar ices [109]. From this result, it is expected that plasma–ice interface can potentially provide a novel reaction field for the laboratory simulation of chemistry that occurs on the ice surfaces in the universe.

Similar to Titan, which appears red in color, icy bodies in the universe may also appear to be of various colors. Particularly, icy bodies in the outer solar system (the re-

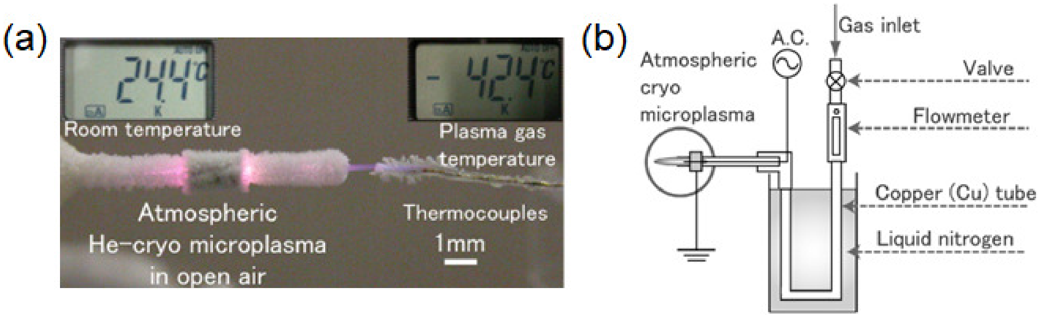

Fig. 14 (a) Atmospheric pressure helium cryoplasma jet generated in open air (applied voltage: AC sinusoidal voltage of 3 kV_{pp}, frequency: 10 kHz, helium flow rate: 1 L min^{-1}). A tungsten wire passed through a quartz capillary was the driving electrode, while a conductive paste coated around the capillary was the ground. Helium gas cooled by liquid nitrogen was introduced into the capillary in which the plasma was generated. Frost was formed around the discharge capillary due to air humidity. Reproduced with permission from [106], copyright 2008 IOP Publishing. (b) Schematic illustration of the setup for the generation of atmospheric pressure helium cryoplasma jet. Reproduced with permission from [106], copyright 2008 IOP Publishing.

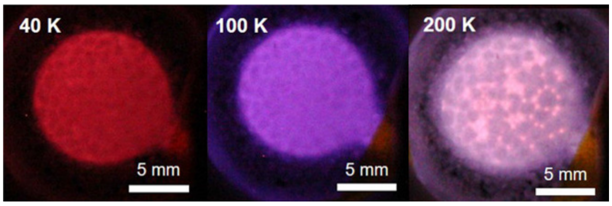

Fig. 15 H_2O-ice dielectric barrier discharge at gas temperature of 200, 100, and 40 K. Reproduced with permission from [108], copyright 2017 IOP Publishing.

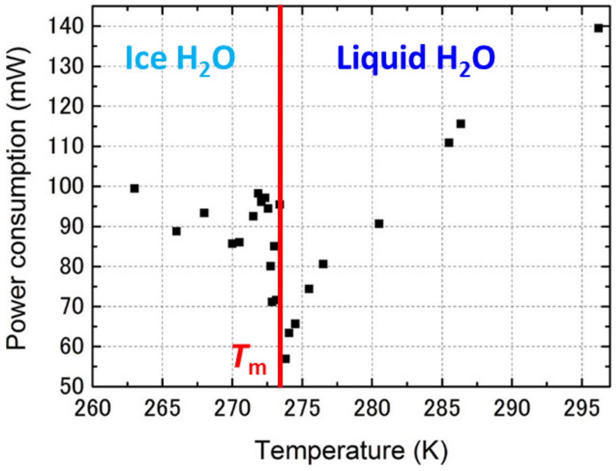

Fig. 16 Power consumption of H_2O-ice dielectric barrier discharge as a function of temperature. Adapted with permission from [108], copyright 2017 IOP Publishing. The temperature ranges for the solid and liquid phases of H_2O have been marked for clarity.

gion of the solar system beyond the asteroid belt which is located between the orbits of Mars and Jupiter), such as trans-Neptunian objects, Kuiper belt objects and Centaurs, can be characterized by their color diversity, which ranges from neutral to ultra-red (see Fig. 17) [110, 111]. Studying the color of such icy bodies that are present in the outer solar system can provide significant clues that shed light on the formation and evolution of the solar system, as they are considered primitive remnants from the early stages of the formation of the solar system [112, 113]. Currently, the reddish coloration of such bodies has been attributed to the reddish-brown complex refractory organic compounds that have been experimentally produced via the irradiation of analog materials [114, 115]. However, such refractory organic compounds are non-volatile at temperatures as high as room temperature, and cannot account for the observational evidence of the absence of ultra-red objects near the sun [118]. Accordingly, the reason behind the color diversity among icy bodies in the outer solar system remains debatable. In our study, which utilizes cryoplasma as an energetic source, we established a reddish coloration of the ice, and the coloration was stable only at cryogenic temperatures. This could provide an alternative explanation to the color diversity of icy bodies present in the outer solar system [116].

Here, the plasma source used was a cryogenic dielectric barrier discharge, which contained helium mixed with 3% nitrogen gas to provide the source of N atoms. One of the dielectric barriers was an ice that comprised a mixture of water (H_2O) and methanol (CH_3OH) (see Fig. 18 (a)), as the source of C atoms. The surface of this ice mixture was irradiated using cryoplasma with 1.75 kV_{pp} sinusoidal A.C. voltage applied at 10 kHz for 12 h at 85 K. The chemicals chosen, namely N_2 and CH_3OH, are considered to be contained in some icy bodies that are present in the outer solar system, while the temperature of 85 K is within the plausible temperature range of the outer solar system. On the other hand, the total energy that was transferred to the ice in this period of irradiation was expected to be of the order of 10^{-3} J $cm^{-2}s^{-1}$, which for instance corresponds to a dose of 10^3 - 10^4 years of energetic radiation on Pluto.

A reddish coloration of the ice that increased in intensity with duration of plasma irradiation, was observed (see Fig. 18 (b)). Upon heating the post-plasma-irradiated

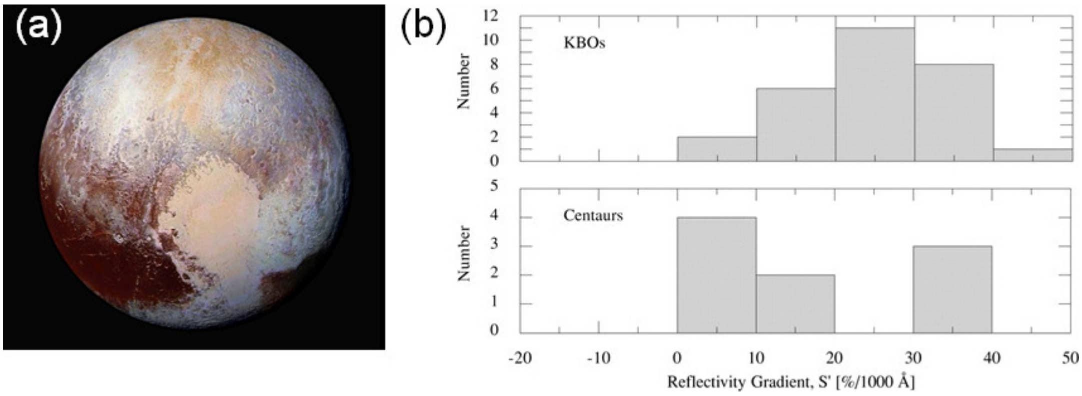

Fig. 17 (a) Color image of Pluto showing a reddish surface [117]. (b) Histograms of the reflectivity gradient, S', for Kuiper belt objects (KBOs) and Centaurs. Here, objects with S'> 25%/1000 Å are defined to be ultrared matter. Reproduced with permission from [118], copyright 2002 The American Astronomical Society.

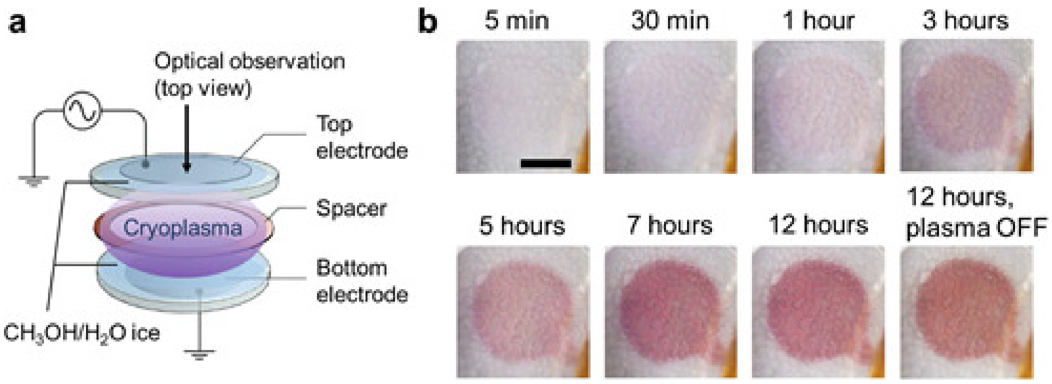

Fig. 18 (a) Schematic illustration of the electrode used. Reproduced with permission from [116], copyright 2020 The American Astronomical Society. (b) Increasing intensity of the reddish coloration of the ice during the plasma irradiation. Reproduced with permission from [116], copyright 2020 The American Astronomical Society. The scale bar is 5 mm.

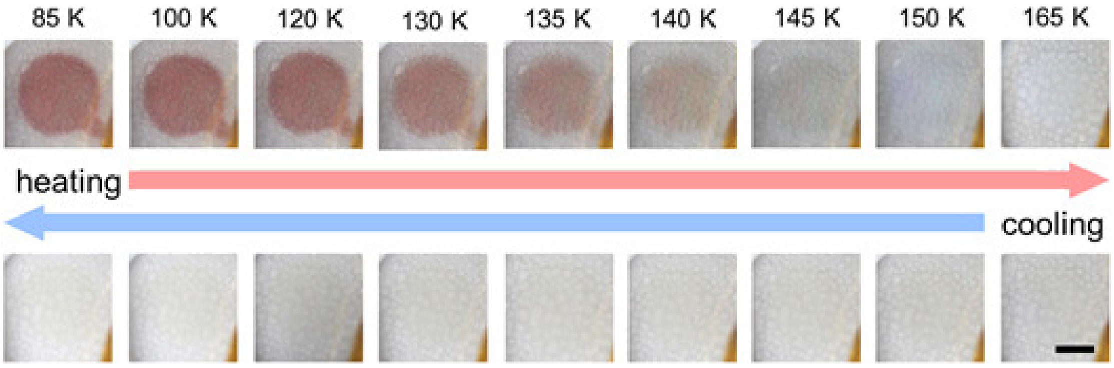

Fig. 19 Fading and irreversible disappearance of the reddish coloration upon heating. Reproduced with permission from [116], copyright 2020 The American Astronomical Society. The scale bar is 5 mm.

ice, the reddish color faded and disappeared at 120 - 150 K (Fig. 19). Therefore, the reddish coloration of the ice was stable only at cryogenic temperatures. The results presented here differ from those presented in previous studies that have attributed the reddish coloration to complex refractory residues, which remain to exist even when heated to room temperature [115, 119].

To analyze the volatiles products formed by the plasma irradiation of ice, temperature programmed desorption (TPD) analysis was performed. The liquid residue after heating the post-plasma-irradiated ice to room temperature was analyzed via liquid chromatograph mass spectroscopy (LC-MS). The synthesis of various organic compounds, such as glycols, carboxylic acids, and

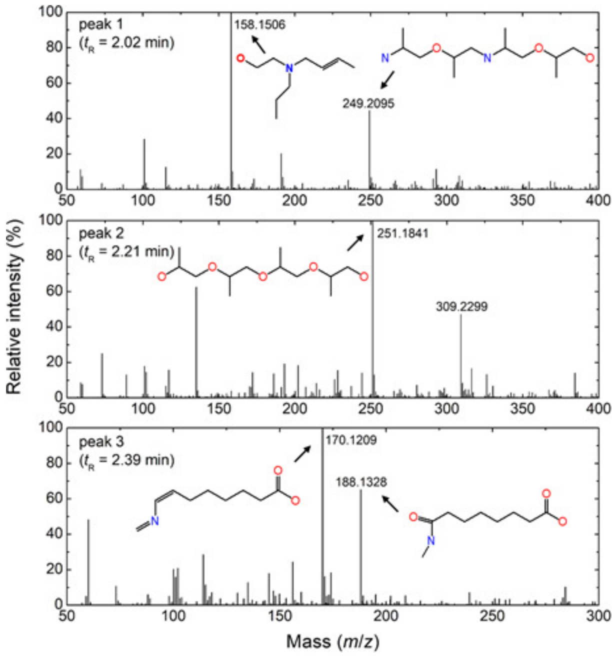

Fig. 20 LC-MS spectra of the room-temperature liquid residue of the plasma-irradiated ice. Reproduced with permission from [116], copyright 2020 The American Astronomical Society.

amides, whose masses were greater than that of the original CH_3OH/H_2O ice was confirmed via LC-MS (see Fig. 20). The presence of compounds that contained C=C and C=N bonds could also be inferred from TPD analyses. The reddish coloration could, tentatively, be explained by these UV- and visible-light-absorbing conjugated systems.

The results of this study showed that the reddish coloration was caused by material that is thermally unstable at high temperatures. This could provide an alternative explanation and experimental support to the idea that ultra-red objects are not found at smaller heliocentric distances, as the reddish materials are thermally unstable at high temperatures. To study the temperature dependence of the ionizing chemistry, further investigations with continuous control of the temperature of the reaction system can be performed; these investigations will help establish the conditions at which such reddish coloration can be formed and sustained. On a wider level, the continuous control of temperature could provide new constraints in understanding the chemical evolution in the low-temperature environment of the universe.

5. Conclusion

In this paper, we presented a short overview of the applications of non-equilibrium low-temperate discharge plasma to the simulations of chemical processes in the domain of astrochemistry. Particularly, we focused on our recent research that utilized cryoplasma, where the temperature of the reaction system could be controlled continuously and precisely below room temperature, to perform laboratory simulations associated with astrochemistry.

Discharge plasma can be used to simulate various chemical processes that occur in the universe. Current research on laboratory simulations that utilize discharge plasma has primarily focused on Titan, which presents an interesting chemistry because it has a nitrogen-dominated atmosphere, which is favorable for organic syntheses. However, apart from Titan, many planetary bodies, as well as other astronomical objects, such as interstellar ices and cometary bodies, are constantly exposed to radiation in the universe. Additionally, lightning activities have been observed on solar system planets, such as Earth, Jupiter, and Saturn [120]. Therefore, in addition to Titan, further research should be conducted on the low-temperature chemistry of other astronomical bodies. We believe that cryoplasma, whose gas temperature can be controlled continuously, is an appropriate energetic source to probe the low-temperature chemistry of a wide range of astrophysical environments that are constantly bombarded by charged and/or excited species. We expect that using cryoplasma as a plasma source in laboratory simulations in the domain of astrochemistry can facilitate the investigation of the temperature dependence of chemical processes, and provide new constraints on the potential chemical species that can be observed in the universe.

[1] E. Herbst and E.F. van Dishoeck, Annu. Rev. Astron. Astrophys. **47**, 427 (2009).
[2] F. Palazzetti *et al.*, J. Chin. Chem. Soc. **59**, 1045 (2012).
[3] A. Ruf *et al.*, Life **8**, 18 (2018).
[4] C.R. Arumainayagam *et al.*, Chem. Soc. Rev. **48**, 2293 (2019).
[5] E.F. van Dishoeck, in *Astrochemistry VII: Through the Cosmos from Galaxies to Planets*, eds. M. Cunningham *et al.*, (Cambridge University Press, Cambridge, 2018) p. 3.
[6] P. Ehrenfreund and S.B. Charnley, Annu. Rev. Astron. Astrophys. **38**, 427 (2000).
[7] E. Herbst, Chem. Soc. Rev. **30**, 168 (2001).
[8] P. Bruston *et al.*, J. Geophys. Res. Planets **99**, 19047 (1994).
[9] M.L. Cable *et al.*, Chem. Rev. **112**, 1882 (2012).
[10] D.P. Cruikshank, in *From Stardust to Planetesimals*, eds. Y.J. Pendleton and A. Tielens (Astronomical Society of the Pacific, San Francisco, 1997) p. 315.
[11] H. Cottin *et al.*, Planet. Space Sci. **47**, 1141 (1999).
[12] P. Coll *et al.*, Adv. Space Res. **16**, 93 (1995).
[13] T.W. Scattergood, Adv. Space Res. **7**, 99 (1987).
[14] D.J. Burke and W.A. Brown, Phys. Chem. Chem. Phys. **12**, 5947 (2010).
[15] S.K. Atreya *et al.*, Planet. Space Sci. **47**, 1243 (1999).
[16] L.E. Snyder, Origins Life Evol. B. **27**, 115 (1997).
[17] I.C.F. Mueller-Wodarg *et al.*, Space Sci. Rev. **139**, 191 (2008).
[18] National Oceanic and Atmospheric Administration, National Aeronautics and Space Administration, and United States Air Force, *U.S. Standard Atmosphere, 1976*, (US Government Printing Office, Washington, D.C.1976).
[19] P.A. Gerakines *et al.*, Icarus **170**, 202 (2004).

[20] S.F.M. Ashbourn *et al.*, Meteorit. Planet. Sci. **42**, 2035 (2007).
[21] C. He and M.A. Smith, Icarus **238**, 86 (2014).
[22] C.J. Bennett *et al.*, Astrophys. J. **660**, 1588 (2007).
[23] C.S. Jamieson *et al.*, Astrophys. J. Suppl. Ser. **163**, 184 (2006).
[24] T. Koike *et al.*, Biol. Sci. Space **17**, 188 (2003).
[25] K.I. Öberg, Chem. Rev. **116**, 9631 (2016).
[26] Y. Takano *et al.*, B. Chem. Soc. Jpn. **77**, 779 (2004).
[27] V. Mennella *et al.*, Astrophys. J. **587**, 727 (2003).
[28] K.K. Sullivan *et al.*, Mon. Not. R. Astron. Soc. **460**, 664 (2016).
[29] M.C. Boyer *et al.*, Surf. Sci. **652**, 26 (2016).
[30] S.M. Hörst, J. Geophys. Res. Planets **122**, 432 (2017).
[31] A. Coustenis and F.W. Taylor, *Titan: Exploring an Earth-like World* (World Scientific, Singapore, 2008).
[32] P.L. Read *et al.*, Q. J. R. Meteorol. Soc. **142**, 703 (2016).
[33] H. Backes *et al.*, Science **308**, 992 (2005).
[34] Y.L. Yung *et al.*, Astrophys. J. Suppl. S. **55**, 465 (1984).
[35] C.P. McKay *et al.*, Planet. Space Sci. **49**, 79 (2001).
[36] C. Szopa *et al.*, Planet. Space Sci. **54**, 394 (2006).
[37] E. De Vanssay *et al.*, Planet. Space Sci. **43**, 25 (1995).
[38] H. Imanaka *et al.*, Icarus **168**, 344 (2004).
[39] H.B. Niemann *et al.*, J. Geophys. Res. Planets **115**, E12006 (2010).
[40] J. Cui *et al.*, Icarus **200**, 581 (2009).
[41] B.A. Magee *et al.*, Planet. Space Sci. **57**, 1895 (2009).
[42] V.A. Krasnopolsky, Icarus **236**, 83 (2014).
[43] M.S. Gudipati *et al.*, Nat. Commun. **4**, 1648 (2013).
[44] T.T. Koskinen *et al.*, Icarus **216**, 507 (2011).
[45] J.H. Waite Jr. *et al.*, Science **316**, 870 (2007).
[46] P.K. Hong *et al.*, Earozoru Kenkyu **31**, 185 (2016).
[47] https://photojournal.jpl.nasa.gov/catalog/PIA17179
[48] Z. Martins *et al.*, Space Sci. Rev. **209**, 43 (2017).
[49] C. He *et al.*, Astrophys. J. Lett. **856**, L3 (2018).
[50] G. Gronoff *et al.*, Astron. Astrophys. **506**, 955 (2009).
[51] M.G. Tomasko *et al.*, in *Huygens: Science, Payload and Mission*, ed. A. Wilson (European Space Agency, Noordwijk, 1997) p. 345.
[52] E. Sciamma-O'Brien *et al.*, Icarus **289**, 214 (2017).
[53] G. Thuillier *et al.*, Sol. Phys. **214**, 1 (2003).
[54] G. Thuillier *et al.*, Metrologia **35**, 689 (1998).
[55] https://www.nasa.gov/mission_pages/shuttle/shuttlemissions/archives/sts-45.html
[56] https://earth.esa.int/web/eoportal/satellite missions/e/eureca
[57] C.P. McKay, Planet. Space Sci. **44**, 741 (1996).
[58] K. Plankensteiner *et al.*, Icarus **187**, 616 (2007).
[59] G. Horvath *et al.*, Plasma Chem. Plasma P. **30**, 565 (2010).
[60] W.R. Thompson *et al.*, Icarus **90**, 57 (1991).
[61] E. Sciamma-O'Brien *et al.*, Icarus **218**, 356 (2012).
[62] A. Mahjoub *et al.*, Plasma Process. Polym. **11**, 409 (2014).
[63] B.N. Khare *et al.*, Icarus **60**, 127 (1984).
[64] J.-M. Bernard *et al.*, Planet. Space Sci. **51**, 1003 (2003).
[65] O. Poch *et al.*, Planet. Space Sci. **61**, 114 (2012).
[66] S.M. Hörst *et al.*, Icarus **301**, 136 (2018).
[67] S.I. Ramírez *et al.*, Faraday Discuss. **147**, 419 (2010).
[68] D. Dubois *et al.*, Icarus **317**, 182 (2019).
[69] M. Fulchignoni *et al.*, Nature **438**, 785 (2005).
[70] N. Carrasco *et al.*, Icarus **219**, 230 (2012).
[71] G.D. McDonald *et al.*, Icarus **108**, 137 (1994).
[72] S. Lebonnois *et al.*, Philos. T. R. Soc. A **367**, 665 (2008).
[73] S. Lebonnois *et al.*, Icarus **152**, 384 (2001).
[74] P. Rannou *et al.*, Adv. Space Res. **36**, 2194 (2005).
[75] R. Moreno *et al.*, Astron. Astrophys. **437**, 319 (2005).
[76] W.B. Hubbard *et al.*, Astron. Astrophys. **269**, 541 (1993).
[77] B. Sicardy *et al.*, J. Geophys. Res. Planets **111**, E11S91 (2006).
[78] A.H. Bouchez, *Seasonal trends in Titan's atmosphere: haze, wind, and clouds* [Ph.D. thesis] (California Inst. of Technol., Pasadena, 2004).
[79] T. Kostiuk *et al.*, Geophys. Res. Lett. **28**, 2361 (2001).
[80] T. Kostiuk *et al.*, Geophys. Res. Lett. **32**, L22205 (2005).
[81] T. Kostiuk *et al.*, J. Geophys. Res. Planets **111**, E07S03 (2006).
[82] D. Luz *et al.*, Icarus **179**, 497 (2005).
[83] D. Luz *et al.*, J. Geophys. Res. Planets **111**, E08S90 (2006).
[84] F.M. Flasar *et al.*, Science **308**, 975 (2005).
[85] C.C. Porco *et al.*, Nature **434**, 159 (2005).
[86] M.K. Bird *et al.*, Nature **438**, 800 (2005).
[87] W.M. Folkner *et al.*, J. Geophys. Res. Planets **111**, E07S02 (2006).
[88] E. Karkoschka, Icarus **270**, 326 (2016).
[89] T. Gautier *et al.*, Icarus **213**, 625 (2011).
[90] P.P. Lavvas *et al.*, Planet. Space Sci. **56**, 67 (2008).
[91] P.P. Lavvas *et al.*, Planet. Space Sci. **56**, 27 (2008).
[92] R.V. Yelle *et al.*, Faraday Discuss. **147**, 31 (2010).
[93] C.N. Keller *et al.*, Planet. Space Sci. **46**, 1157 (1998).
[94] D. Dubois *et al.*, Icarus **338**, 113437 (2020).
[95] N. Carrasco *et al.*, Int. J. Chem. Kinet. **40**, 699 (2008).
[96] P. Coll *et al.*, Planet. Space Sci. **47**, 1433 (1999).
[97] E. Sciamma-O'Brien *et al.*, Icarus **243**, 325 (2014).
[98] N. Fray and B. Schmitt, Planet. Space Sci. **57**, 2053 (2009).
[99] G.D. McDonald *et al.*, Icarus **122**, 107 (1996).
[100] C.G. Justus and R.D. Braun, NASA article, https://ntrs.nasa.gov/archive/nasa/casi.ntrs.nasa.gov/20070032693.pdf (2007).
[101] A. Seiff *et al.*, J. Geophys. Res. Planets **103**, 22857 (1998).
[102] G.F. Lindal *et al.*, J. Geophys. Res. Space Phys. **92**, 14987 (1987).
[103] K. Lodders and B. Fegley Jr., *The Planetary Scientist's Companion* (Oxford University Press, New York1998).
[104] J. Klinger, Icarus **47**, 320 (1981).
[105] S. Stauss *et al.*, Plasma Sources Sci. Technol. **27**, 023003 (2018).
[106] D. Ishihara *et al.*, Plasma Sources Sci. Technol. **17**, 035008 (2008).
[107] Y. Noma *et al.*, Appl. Phys. Lett. **93**, 101503 (2008).
[108] N. Sakakibara and K. Terashima, J. Phys. D Appl. Phys. **50**, 22LT01 (2017).
[109] G.M.M. Caro *et al.*, Nature **416**, 403 (2002).
[110] P. Lacerda *et al.*, Astrophys. J. Lett. **793**, L2 (2014).
[111] N. Peixinho *et al.*, Astron. Astrophys. **410**, L29 (2003).
[112] A. Doressoundiram *et al.*, Icarus **154**, 277 (2001).
[113] T. Montmerle *et al.*, Europ. Astronom. Soc. Publ. Ser. **41**, 325 (2010).
[114] D.P. Cruikshank *et al.*, Adv. Space Res. **36**, 178 (2005).
[115] C.K. Materese *et al.*, Astrophys. J. **812**, 150 (2015).
[116] N. Sakakibara *et al.*, Astrophys. J. Lett. **891**, L44 (2020).
[117] S.A. Stern *et al.*, Science **350**, aad1815 (2015).
[118] D.C. Jewitt, Astron. J. **123**, 1039 (2002).
[119] C.K. Materese *et al.*, Astrophys. J. **788**, 111 (2014).
[120] C. Helling, J. Phys. Conf. Ser. **1322**, 012028 (2019).